

Line-mixing in the $^{\ell}Q$ sub branches of the ν_1 band of methyl chloride

C. Bray^{a,b,*}, *H. Tran*^c, *D. Jacquemart*^{a,b}, *N. Lacome*^{a,b}

^aUPMC Univ Paris 06, Laboratoire de Dynamique, Interactions et Réactivité, UMR 7075,
Case Courrier 49, 4 Place Jussieu, 75252 Paris Cedex 05, France

^bCNRS, UMR 7075, Laboratoire de Dynamique, Interactions et Réactivité, Case Courrier 49,
4 Place Jussieu, 75252 Paris Cedex 05, France

^cLaboratoire Interuniversitaire des Systèmes Atmosphériques, UMR CNRS 7583, Université
Paris Est Créteil (UPEC) et Université Paris Diderot (UPD). Université Paris Est Créteil, 61
avenue du Général de Gaulle, 94010 Créteil Cedex, France

Number of Figures: 5

Number of Tables: 3

Please send proofs to: Bray Cédric

* corresponding author : Cédric Bray (Email: bray@spmol.jussieu.fr)

Tel. 33 (0)1 44 27 36 82 - Fax: 33 (0)1 44 27 30 21

Keywords : methyl chloride; ν_1 band; High-resolution Fourier Transform spectra; room
temperature; line-mixing; vibration rotation.

Abstract

Line-mixing effects have been studied in the $\nu_1 \ ^Q Q_K$ (K from 0 to 10) sub branches of methyl chloride (CH_3Cl) perturbed by nitrogen (N_2). Laboratory Fourier transform spectra have been recorded at room temperature for various pressures of atmospheric interest. In order to accurately model these spectra, a theoretical approach accounting for line-mixing effects is necessary and proposed in this study. The common model used in this work is based on the state-to-state rotational cross-sections calculated by a statistical modified exponential-gap fitting law depending on few empirical parameters. These parameters have been deduced by least-squares fitting a sum rule to the N_2 -broadening coefficients modeled previously. Comparisons between experimental and calculated spectra for various $\ ^Q Q$ sub branches and various pressures of N_2 demonstrate the adequacy of the model as compared to the use of the Voigt profile.

1. Introduction

Methyl chloride (CH_3Cl) is one of the most abundant chlorine-containing molecules in the earth atmosphere. It has a rather strong signature around 3000 cm^{-1} (especially the ν_1 band) which was recently used by the Atmospheric Chemistry Experiment (ACE) satellite mission to produce the first global distribution of methyl chloride in the upper troposphere and stratosphere [1]. This spectral region has been recently studied, for transitions of both $\text{CH}_3^{35}\text{Cl}$ and $\text{CH}_3^{37}\text{Cl}$ isotopologues, in terms of line positions and intensities [2], self- [3] and N_2 -broadening coefficients [4].

$^Q Q$ sub branches of the ν_1 band are used for atmospheric remote sensing in this region since they are quite strong and in a relatively transparent window. Under atmospheric conditions, line-mixing effects can be observed since the structure of these branches is narrow [5]. In the following, it is shown that the line mixing effects in the $^Q Q$ sub branches must be taken into account for accurate atmospheric applications. Line-mixing effects were disregarded in our previous studies [2-4], since low pressures of CH_3Cl or N_2 (lower than 120 mbar) spectra were used. In the present work, nitrogen (N_2) pressures up to 700 mbar are considered. In such conditions, the usual Voigt or Lorentz profiles cannot correctly reproduce the experimental shape of the $^Q Q$ sub branches. Note that, for CH_3Cl , line-mixing has been previously studied for the $^R Q_0$ sub-branches of the ν_5 band [6-8], but never for the ν_1 band. In this work, a model has been used to calculate line-mixing for the $^Q Q_K$ (K from 0 to 10) sub-branches of the ν_1 band of CH_3Cl perturbed by N_2 . This model is based on the use of the state-to-state rotational cross-sections and a statistical Exponential Power Gap (EPG) fitting law depending on few empirical parameters.

Laboratory Fourier transform spectra have been recorded at room temperature and for 3 pressures of N_2 (between 200 and 700 mbar). Line mixing effects are observed in the $^Q Q$ sub-branches, and increased with the pressure of N_2 . Experimental conditions are presented in Section 2. Section 3 is devoted to the line mixing model. Comparisons between experimental and calculated spectra are discussed in Section 4.

2. Experimental conditions

The rapid scan Bruker IFS 120 HR interferometer of the Laboratoire de Dynamique, Interactions et Réactivité (LADIR) was used to record N_2 -perturbed spectra of CH_3Cl . The

unapodized spectral resolution (FWHM) used was about $25 \times 10^{-3} \text{ cm}^{-1}$, corresponding to a maximum optical path difference of 20 cm. Such a resolution is sufficient enough to neglect the apparatus function in the calculation because of the strong width (around 0.2 cm^{-1} at 1 atm of N_2) of the $^Q Q$ sub branches of CH_3Cl . The interferometer was equipped with a CaF_2 beamsplitter, an InSb detector and a Globar source. The experimental conditions of the recorded spectra are summarized in Table 1. Under these conditions, the rotational structure of CH_3Cl transitions is not resolved, as can be observed in Fig. 1, which presents the various $^Q Q$ sub branches studied in this work. For all spectra, the whole optical path was under vacuum. A multipass cell of 1m base length, with a total absorption path of 415 cm, was used. This cell was equipped with KCl windows. The commercial gas sample of CH_3Cl and N_2 , furnished by Alpha gas with a stated purity of 99.9% in natural abundances (74.89 % of $^{12}\text{CH}_3^{35}\text{Cl}$ and 23.94 % of $^{12}\text{CH}_3^{37}\text{Cl}$), was used without further purification. The temperature in the cell was recorded using four platinum probes inside the cell. The spectra were recorded at room temperature (see Table 1). Pressures of gases have been measured with two Baratron gauges with accuracy better than $\pm 0.15 \%$ for the 1 mbar full scale gauge and better than $\pm 0.25 \%$ for the 1000 mbar full scale gauge. Around 400 scans have been averaged and then transformed to spectrum, using the Fourier transform procedure included in the Bruker software OPUS package [9], selecting a Mertz phase-error correction [10,11]. The spectra were not numerically apodized. Averaging the 400 scans, the signal-to-noise ratio was nearly equal to 600. Note that, a weak multiplicative channel spectrum was expected in the experimental spectra due to the reflexion on parallel faces of windows in the experimental set up (1% maximum peak to peak amplitude). Due to the high pressures of gas used in this work, this channel cannot be observed in the spectral range of the CH_3Cl absorption features. In this study, the pressure broadening width leads to intrinsic non resolved transitions, especially for the $^Q Q$ sub branches, so that, the multiplicative channel was hidden behind. Consequently, spectra were divided by a vacuum spectrum to eliminate this channel.

3. Line-mixing calculation

This section is dedicated to the calculation used to evaluate line-mixing effects in $\text{CH}_3\text{Cl}/\text{N}_2$ spectra for $^Q Q$ sub-branches of ν_1 band. Sections 3.1 and 3.2 are devoted to the formulation of the absorption coefficient and of the relaxation operator respectively. The calculation of CH_3Cl spectra perturbed by N_2 under the experimental conditions given in Table 1 is described in Section 3.3.

3.1. Absorption coefficient

Let us consider a mixture of two gases, an absorbing gas (noted a) and a buffer gas (noted b). Within the impact and binary collisions approximations, and disregarding Doppler effect, which has negligible influences in the studied pressure range, the absorption coefficient α (in cm^{-1}) accounting for line-mixing effects at a wavenumber σ is given by [12,13] (Note that the CGS unit system is used for all the quoted equations):

$$\alpha(\sigma, P_a, P_b, T) = \frac{8\pi^2\sigma}{3hc} [1 - \exp(-hc\sigma / k_b T)] P_a \sum_k \sum_l \rho_k(T) d_k d_l \times \text{Im} \left\langle \left\langle l \left| \left[\Sigma - L_0 - i(P_a \mathbf{W}_{a/a}(T) + P_b \mathbf{W}_{a/b}(T)) \right]^{-1} \right| k \right\rangle \right\rangle, \quad (1)$$

(rajouter {} après Im)

where P_a and P_b are the partial pressures of the absorbing and buffer gases, respectively, and T the temperature of the gas. The sums include all absorption lines k and l ; $\text{Im}\{\dots\}$ denotes the imaginary part; ρ_k is the relative population of the initial level of line k , d_n is the reduced matrix element of the electric dipole moment operator of line n ($n = l$ or k), related to the integrated line intensity S_n of the absorbing gas by:

$$S_n(T) = \frac{8\pi^3}{3hc} \rho_n(T) \sigma_n [1 - \exp(-hc\sigma_n / k_b T)] d_n^2. \quad (2)$$

k_b is the constant of Boltzmann. Σ , L_0 and \mathbf{W} are operators in the Liouville line space. The first two are diagonal and can be expressed as follows:

$$\langle \langle l | \Sigma | k \rangle \rangle = \sigma \delta_{k,l} \quad \text{and} \quad \langle \langle l | L_0 | k \rangle \rangle = \sigma_k \delta_{k,l}, \quad (3)$$

$\delta_{k,l}$ being the Kronecker symbol. The relaxation operators $\mathbf{W}_{a/a}$ and $\mathbf{W}_{a/b}$, which contain the influence of collisions on the spectral shape, depend on the band and on the temperature. The off-diagonal elements of \mathbf{W} account for interferences between absorption lines (line mixing), whereas the real and imaginary parts of the diagonal elements are the pressure-broadening γ_k and pressure-shifting coefficients δ_k of the lines

$$\langle \langle k | \mathbf{W}(T) | k \rangle \rangle = \gamma_k(T) - i\delta_k(T). \quad (4)$$

3.2. Relaxation operator

According to Eq. (4), the diagonal elements of \mathbf{W} are directly linked to the broadening and shifting coefficients of the transitions involved in line mixing calculation. Since no N_2 shifting coefficient of CH_3Cl is available in this region, they have been neglected in this study. Therefore, the imaginary part of the off-diagonal elements has also been disregarded.

The real off-diagonal elements are modeled using the state-to-state inelastic collisional rates of the lower state through:

$$\langle\langle l|\mathbf{W}(T)|k\rangle\rangle = -A_{l,k}K(i_l \leftarrow i_k, T) \text{ with } (i_l \neq i_k), \quad (5)$$

where $K(i_l \leftarrow i_k, T)$ designates the state-to-state collisional transfer rate from the initial level i_k of line k to the initial level i_l of line l . The parameters $A_{l,k}$, which enable switching from the state space to the line space, are empirical and depend on the types of considered lines [14,15]. In order to simplify the problem, we made the approximation that $A_{l,k}$ depends only on the band and on the buffer gas, but not on the quantum numbers of the lines themselves.

The downward rates $K(i_l \leftarrow i_k, T)$, with $E_l < E_k$, are modeled by a statistical Exponential Power Gap (EPG) fitting law [10,13,16]:

$$K(i_l \leftarrow i_k, T) = a_1 |E_k - E_l|^{-a_2} e^{-a_3 |E_k - E_l|}, \quad (6)$$

where E_n is the rotational energy of the initial level of line n ($n = l$ or k). The coefficients a_1 , a_2 and a_3 are empirical parameters.

The upward rates are then calculated by using the detailed balance:

$$K(i_k \leftarrow i_l, T) = \frac{\rho_k(T)}{\rho_l(T)} K(i_l \leftarrow i_k, T). \quad (7)$$

The coefficients a_1 , a_2 and a_3 in Eq. (6) are obtained by least-squares fitting the sum rule to the N_2 -broadening coefficients γ_k values. For a ${}^Q Q$ sub branch, this sum rule is given by:

$$\gamma_k = \frac{1}{2} \left[\sum_{i_k \neq i_l} K(i_l \leftarrow i_k) + \sum_{f_k \neq f_l} K(f_l \leftarrow f_k) \right], \quad (8)$$

where i_n and f_n are, respectively, the initial and final levels of the transition n ($n = l$ or k).

3.3. Application to the CH_3Cl spectra

Using experimental conditions of Table 1 and the model previously described, the line mixing due to N_2 pressure has been calculated in the various ${}^Q Q_K$ (K from 0 to 10) sub branches of the ν_1 band. As these ${}^Q Q$ sub branches are well separated (see Fig. 1), inter-branch line mixing (for example with $\Delta K=3n$ [17]) has not been taken into account.

The spectroscopic parameters of the line k required for the calculation of the spectra are the position σ_k , the relative population of the initial level ρ_k , the reduced matrix element of the electric dipole moment operator d_k (obtained from S_k), the rotational energy level E_k ,

and the N₂-broadening coefficients γ_k . All these parameters have been constrained to the calculated values obtained in Refs. [2-4]. Since partial pressure of methyl chloride is very small (around 0.25 mbar), self-broadening contribution has been neglected. The contributions of the ¹³C species (concentration of about 1%) were also neglected. Note that the whole absorption coefficient is the sum of the absorption coefficients due to each isotopologues and that the line intensity in Eq. (2) is defined for a pure gas, not to be confused with those given in natural abundances in Ref. [2].

For the calculation of the off-diagonal elements of the relaxation operators W_{CH_3Cl/N_2} , the parameters a_1 , a_2 and a_3 have been adjusted using Eq. (6), the calculated N₂-broadening coefficients of Ref. [4], and the sum rule given in Eq. (8). For this, the values of the broadening coefficients obtained by an empirical model in Ref. [4] were chosen, instead of the measured values. The N₂-broadening coefficients have been calculated with the empirical model of Ref. [4] from J equal 0 to 50 and K equal 0 to 9. Since in Ref. [4] no evident discrepancy has been observed between the N₂-broadening coefficients of CH₃³⁵Cl and CH₃³⁷Cl, the a_1 , a_2 and a_3 parameters are the same for both isotopologues. The parameters a_1 , a_2 and a_3 have been obtained for the most intense oQ_6 sub branch, and were retained for all the other oQ sub branches.

The vibrational ground state has only A+ levels. The upper states of oQ_6 transitions are split into A- and A+ levels. The optical selection rule for these oQ_6 transitions is A+↔A-. As mentioned by Chackerian et al. [8], collisional relaxation between both A-↔A- and A+↔A- levels (instead of only A-↔A-) in the excited state were needed to correctly describe line-mixing effects in the RQ_0 sub branch of the ν_5 band of CH₃Cl. In this case, the sum rule becomes:

$$\gamma_k = \frac{1}{2} \left[\sum_{i_k \neq i_l} K(i_l \leftarrow i_k) + \frac{1}{2} \sum_{\substack{f_k \neq f_l \\ A \leftrightarrow A^+}} K(f_l \leftarrow f_k) + \frac{1}{2} \sum_{\substack{f_k \neq f_l \\ A \leftrightarrow A^-}} K(f_l \leftarrow f_k) \right]. \quad (9)$$

However, in the case of the oQ sub branch of the ν_1 band of CH₃Cl, the rotational energies of A- and A+ levels of the upper state are very close, so that this refinement does not change the value of the right member of Eq. (8). Therefore, only A-→A- collisional relaxations in the upper state have been considered to simplify the calculation. Consequently Eq. (9) becomes:

$$\gamma_k = \frac{1}{2} \left[\sum_{i_k \neq i_l} K(i_l \leftarrow i_k) + \sum_{\substack{f_k \neq f_l \\ A^- \leftrightarrow A^-}} K(f_l \leftarrow f_k) \right]. \quad (10)$$

For the oQ_6 sub-branch, the sum rule was evaluated with unrestricted collisional selection rules on ΔJ , with J_k of the lower state lesser or equal to 35 and with J_l of the upper state up to 50 (in order to ensure the convergence of the rule sum [Eq. (10)]) and with $\Delta K=0$ [17,19-21].

The values obtained for the a_1 , a_2 , and a_3 coefficients are given in Table 2, and the validity of the model is demonstrated in Fig. 2, showing the comparison between the N_2 -broadening coefficients calculated in such a way and the values from Ref. [4]. The coefficient $A_{l,k}$ in Eq. (5) was determined from one single experimental spectrum (spectre 3 of Table 1). This was done by successive estimations, and we found that the coefficient $A_{N_2} = 0.55$ was the optimum value to reproduce both sub branches at the three experimental pressures. For all oQ sub branches, the relaxation operators W_{CH_3Cl/N_2} were then calculated from the set of parameters of Table 2, using Eqs. (5-7) and using the parameter A_{N_2} . The broadening parameters calculated from the off-diagonal elements and the sum rule does not match perfectly (see Fig. 2) especially for the other oQ sub branches for which the broadening coefficients for $K=6$ differs from those at other K values. Consequently a renormalization procedure [18] was applied to the off-diagonal terms for each branch, in order to satisfy exactly the sum rule and the K rotational dependence of the N_2 -broadening coefficients. Finally, note that the calculation of spectra was performed by the direct calculation of Eq. (1) through the inversion of the relaxation operators W_{CH_3Cl/N_2} .

4. Spectra calculations and discussion

Due to the broadened unresolved structure of the oQ branches (about 0.2 cm^{-1} at 1 atm), it was not necessary to take into account the effect of apparatus function. Absorption coefficients due to the two $CH_3^{35}Cl$ and $CH_3^{37}Cl$ isotopologues were added. Uncoupled lines present in the studied spectral domains were also taken into account in the calculation of the total absorption coefficient, their contribution being calculated using a Lorentz profile. Because of the high pressures, it was not necessary to take into account the Doppler broadening for CH_3Cl in this spectral region. Moreover, due to the low pressures of CH_3Cl used in this work, the effect of the self-broadening coefficients has been neglected. In the studied spectral region, the Doppler width is about 0.0025 cm^{-1} , whereas in spectrum 1 (see table 1) the self-width is equal to 0.0002 cm^{-1} , while the N_2 -width is equal to 0.04 cm^{-1} .

Using the a_1 , a_2 , and a_3 parameters reported in Table 2 for N_2 -perturbed CH_3Cl and the value $A_{N_2} = 0.55$, calculation with and without line mixing effect were performed. The results obtained for the oQ_6 sub branches at the three pressures of Table 1 are presented in Fig. 3. The residuals can achieve 30% when not introducing line-mixing effects, whereas it achieved only 6% when taking this effect into account with our model. The spectra calculated for the other oQ sub branches are shown in Fig. 4. Let us recall that the renormalization procedure was necessary for these branches, since the model parameters were obtained from the oQ_6 sub branch only. As can be observed in Fig. 4, line-mixing effects are quite important for all sub branches and our calculation significantly improves the residual as compared to a calculation without line mixing. Table 3 shows the maximum residual in percent for each branch when performing line mixing calculation or using a Lorentz profile. A slight systematic residual increasing with K is observed. This difference can be due to a K dependence of line-mixing effects not introduced in our W_{CH_3Cl/N_2} calculation since the A coefficient is constant for all oQ sub branches, and to the fact that N_2 pressure-shift has been neglected. For branches with high K values ($K > 8$), less accurate spectroscopic data can also explain the more important residual. These results confirm that neglecting line mixing leads to large errors, whereas our model gives better predictions.

A comparison between a calculated spectrum based on the line parameters of Refs. [2-4] and the experimental spectrum of the Pacific Northwest National Laboratory (PNNL) [22] is shown in Fig. 5. The PNNL spectrum was recorded at 0.001 mbar of CH_3Cl and 1013 mbar of N_2 . Under these conditions, the calculated spectrum presents strong effect of line mixing as it can be observed on this figure. The improvement on the calculation when the line mixing is taking into account is significant. For atmospheric retrievals from the oQ sub branches of the ν_1 band of CH_3Cl , the use of line parameters from databases [23-24] or from Refs. [2-4] is not sufficient since neglecting line-mixing effects will introduce systematic errors in the retrieval of the CH_3Cl abundance.

5. Conclusion

Line-mixing effects have been calculated for the oQ sub branches (up to $K = 10$) of the ν_1 band of methyl chloride (CH_3Cl), perturbed by N_2 (200-700 mbar) at room temperature. The model is based on the use of the state-to-state rotational cross-sections calculated by a statistical modified exponential-gap fitting law that depends on a few adjusted empirical parameters. Comparisons performed between experimental and calculated spectra

demonstrate the effectiveness of the model as compared to the use of a Voigt or Lorentz profile. The influence of line-mixing effects on the abundance of CH₃Cl is important for atmospheric retrievals. All programs and results that are required to calculate the line mixing for oQ sub branches of the ν_1 band of CH₃Cl are available upon request to the authors.

Acknowledgments

Dr. J.-M. Hartmann and Dr. A. Perrin are gratefully acknowledged for very helpful suggestions and discussions throughout this work.

References

- [1] Kaley AW, Weigum N, McElcheran C, Taylor JR. Global methyl chloride measurements from the ACE-FTS instrument. International Symposium on Molecular Spectroscopy Department of Chemistry The Ohio State University, TI-09; 2009.
- [2] Bray C, Perrin A, Jacquemart D, Lacombe N. The ν_1 , ν_4 and $3\nu_6$ bands of methyl chloride in the 3.4 μm region: line positions and intensities. JQSRT 2011;112:2446-62.
- [3] Bray C, Jacquemart D, Lacombe N, Guinet M, Cuisset A, Eliet S, Hindle F, Mouret G, Rohart F, Buldyreva J. Self-broadening coefficients of methyl chloride transitions at room temperature. Submitted in JQSRT.
- [4] Bray C, Jacquemart D, Buldyreva J, Lacombe N, Perrin A. The N_2 -broadening coefficients of methyl chloride at room temperature. JQSRT 2012;113:1102-12.
- [5] Hartmann JM, Boulet C, Robert D. Collisional effects on molecular spectra. Elsevier; 2008.
- [6] Hartmann JM, Bouanich JP, Boulet C, Blanquet G, Walrand J, Lacombe N. Simple modelling of Q branch absorption-II: application to molecules of atmospheric interest (CFC-22 and CH_3Cl). JQSRT 1995;54:723-35.
- [7] Frichot F, Lacombe N, Hartmann JM. Pressure and temperature dependences of absorption in the ν_5 RQ_0 branch of CH_3Cl in N_2 : measurements and modelling. J Mol Spectrosc 1996;178:52-8.
- [8] Chackerian Jr. C, Brown LR, Lacombe N, Tarrago G. Methyl chloride ν_5 region lineshape parameters and rotational constants for the ν_2 , ν_5 , and $2\nu_3$ vibrational bands. J Mol Spectrosc 1998;191:148-57.
- [9] Wartewig S. IR and Raman spectroscopy: fundamental processing. Weinheim: Wiley-VCH; 2003.
- [10] Mertz L. Transformations in optics. New York: Wiley; 1965.
- [11] Griffiths PR, deHaseth JA. Fourier transform infrared spectrometry. New York: Wiley; 1986.
- [12] Ben-Reuven A. Impact broadening of microwave spectra. Phys Rev 1966;145:7-22.
- [13] Lévy A, Lacombe N, Chackerian Jr. C. Collisional line-mixing. In: Rao KN, Weber A, editors. Spectroscopy of the Earth's atmosphere and interstellar medium. New York: Academic Press, Inc.; 1992. p. 261-337.
- [14] Pieroni D, Nguyen Van T, Brodbeck C, Claveau C, Valentin A, Hartmann JM, et al. Experimental and theoretical study of line-mixing in methane spectra. I. The N_2 -broadened ν_3 band at room temperature. JQSRT 1999;110:7717-32.

- [15] Tran H, Flaud PM, Gabard T, Hase F, von Clarmann T, Camy-Peyret C, Payan S, Hartmann JM. Model, software and database for line-mixing effects in the ν_3 and ν_4 bands of CH_4 and tests using laboratory and planetary measurements-I: N_2 (and air) broadening and the Earth atmosphere. *JQSRT* 2006;101:284–305.
- [16] Rahn LA, Palmer RE. Studies of nitrogen self-broadening at high temperature with inverse Raman spectroscopy. *J Opt Soc Am B* 1986;3:1164–9.
- [17] Herlemont F, Thibault J, Lemaire J. Study of rotational relaxation in CH_3Br by infrared–microwave double resonance. *Chem Phys Lett* 1976;41:466–9.
- [18] Niro F, Boulet C, Hartmann JM. Spectra calculations in central and wing region of CO_2 IR bands between 10 and 20 mm-I: model and laboratory measurements. *JQSRT* 2004;88:483–98.
- [19] Everitt HO, de Lucia F. Rotational energy transfer in CH_3F : the $\Delta J=n$, $\Delta f=0$ processes. *J Chem Phys* 1990;92:6480–91.
- [20] Frenkel L, Marantz H, Sullivan T. Spectroscopy and collisional transfer in CH_3Cl by microwave–laser double resonance. *Phys Rev A* 1971;3:1640–51.
- [21] Pape TW, De Lucia FC, Skatrud DD. Time resolved double resonance study of J and K changing rotational collision processes in CH_3Cl . *J Chem Phys* 1994;100:5666–83.
- [22] Sharpe SW, Johnson TJ, Sams RL, Chu PM, Rhoderick GC, Johnson PA. Gas-Phase Databases for Quantitative Infrared Spectroscopy. *Appl Spectrosc* 2004; 58:1452-61.
- [23] Rothman LS, Gordon IE, Barbe A, Benner DC, Bernath PF, Birk M, Boudon V, Brown LR, Campargue A, Champion JP, Chance K, Coudert LH, Dana V, Devi VM, Fally S, Flaud JM, Gamache RR, Goldman A, Jacquemart D, Kleiner I, Lacombe N, Lafferty QJ, Mandin JY, Massie ST, Mikhailenko SN, Miller CE, Moazzen-Ahmadi N, Naumenko OV, Nikitin AV, Orphal J, Perevalov VI, Perrin A, Predoi-Cross A, Rinsland CP, Rotger M, Simeckova M, Smith MAH, Sung K, Tashkun SA, Tennyson J, Toth RA, Vandaele AC, Vander Auwera J. The HITRAN 2008 molecular spectroscopic database. *JQSRT* 2009;110:533–72.
- [24] Jacquinet-Husson N, Scott NA, Chédin A, Crépeau L, Armante R, Capelle V, Orphal J, Coustenis A, Barbe A, M. Birk, Brown LR, Camy-Peyret C, Claveau C, Chance K, Christidis N, Clerbaux C, Coheur PF, Dana V, Daumont L, Debacker-Barilly MR, Di Lonardo G, Flaud JM, Goldman A, Hamdouni A, Hess M, Hurley MD, Jacquemart D, Kleiner I, Köpke P, Mandin JY, Massie S, Mikhailenko S, Nemtchinov V, Nikitin A, Newnham D, Perrin A, Perevalov VI, Pinnock S, Régalia-Jarlot L, Rinsland CP, Rublev A, Schreier F, Schult L, Smith KM, Tashkun SA, Teffo JL, Toth RA, Tyuterev VI, Vander Auwera J, Varanasi P, Wagner G, The GEISA spectroscopic database: Current and future archive for Earth’s planetary atmosphere studies. *JQSRT* 2008;109:1043-59.

Table 1

Experimental conditions of the recorded spectra.

#	CH ₃ Cl pressure (mbar)	N ₂ pressure (mbar)	Resolution ^a (cm ⁻¹)	Temperature (K)
1	0.2562	218.6	0.02	294.3 ±0.5
2	0.2706	409.8	0.05	293.5 ±0.5
3	0.2640	698.2	0.05	297.0 ±0.5

^a Resolution as defined by Bruker = 0.9/Maximum optical path

Table 2
Parameters of the EPG model (Eq. 7) obtained for CH₃Cl/N₂.

EPG law parameter	CH ₃ Cl/N ₂
a_1	0.067
a_2	0.584
a_3	0.764

Table 3

Residual in percent for each branch when line mixing is taken or not into account for the spectrum 3.

Branch of ν_1 band	Obs-calc* Without line mixing (%)	Obs-calc* With line mixing (%)
oQ_1	-10.6	-0.9
oQ_2	-21.4	-1.5
oQ_3	-27.7	5.1
oQ_4	-29.3	4.4
oQ_5	-34.0	-1.2
oQ_6	-29.1	-5.6
oQ_7	-37.9	-9.1
oQ_8	-36.5	-9.2
oQ_9	-35.8	-18.5
${}^oQ_{10}$	-37.3	-18.7

* Difference at the maximum peak absorption ($\% = \frac{T_{obs} - T_{calc}}{1 - T_{obs}} \times 100$, T_{obs} and T_{calc} correspond to the transmittance of the experimental and calculated spectra, respectively)

Figure 1

On left side, in the upper panel, the experimental spectrum 1 (see Table 1) is plotted. The panels of residuals show the differences between the experimental spectrum and a spectrum calculated without taking into account line-mixing (a) and with line mixing taken into account (b). On right side, a zoom of the oQ sub branches is plotted. K -rotational structure of sub branches is resolved contrary to the J -rotational structure of each branch. Note also that the oQ sub branches of the two isotopologues of ${}^{12}\text{CH}_3\text{Cl}$ are not resolved.

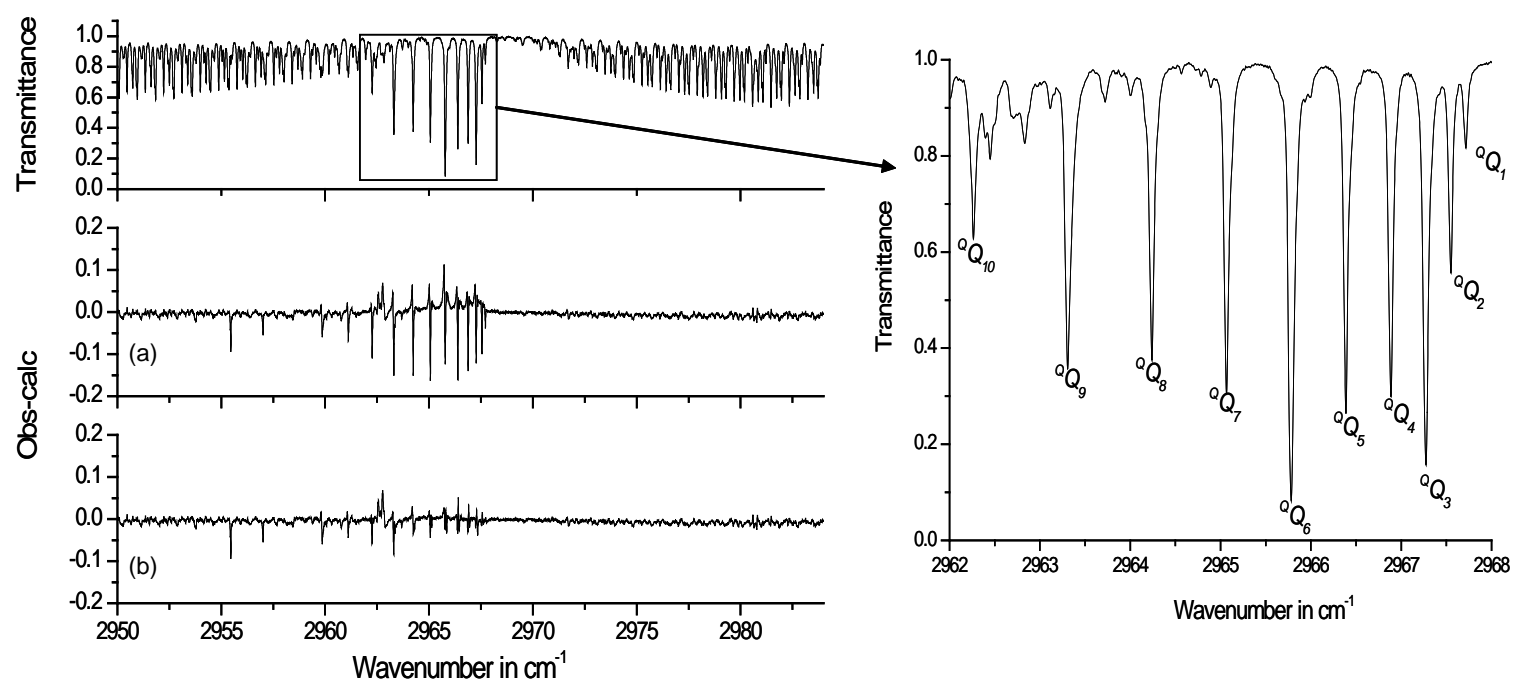


Figure 2

Comparison between N_2 -broadening coefficients of CH_3Cl in the oQ_6 sub branch given by the empirical model of [4] (solid square) and those calculated using the EPG model and coefficients of Table 2 (solid curve). Note that the broadening coefficients calculated for $CH_3^{35}Cl$ and $CH_3^{37}Cl$ are not distinguishable from the solid curve shown. J is the rotational quantum number of the lower level of the transition.

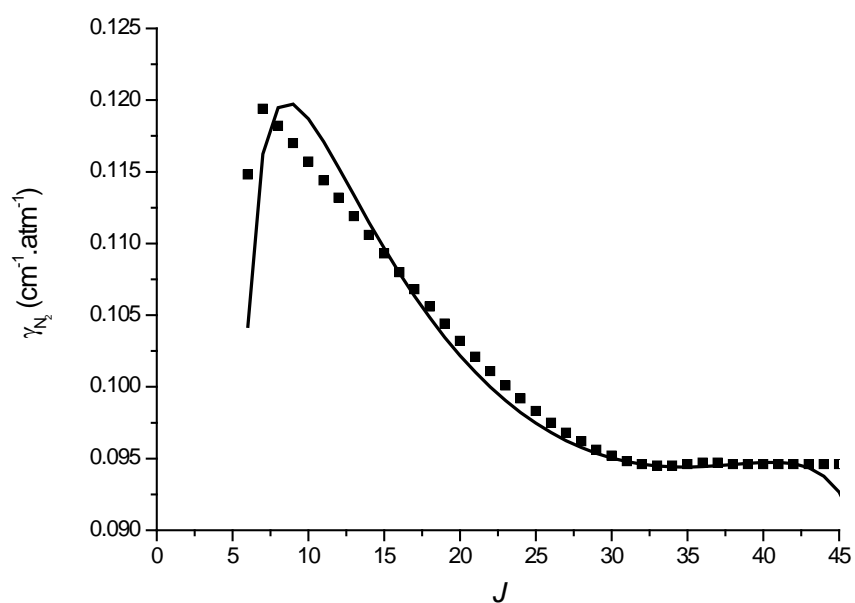
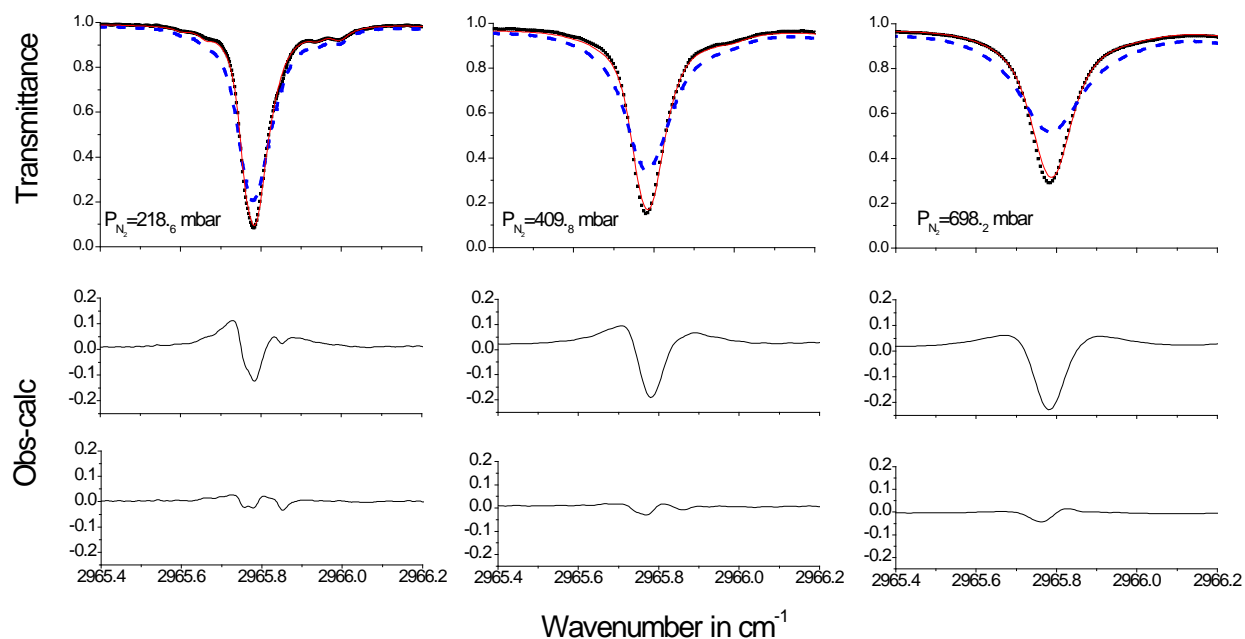


Figure 3

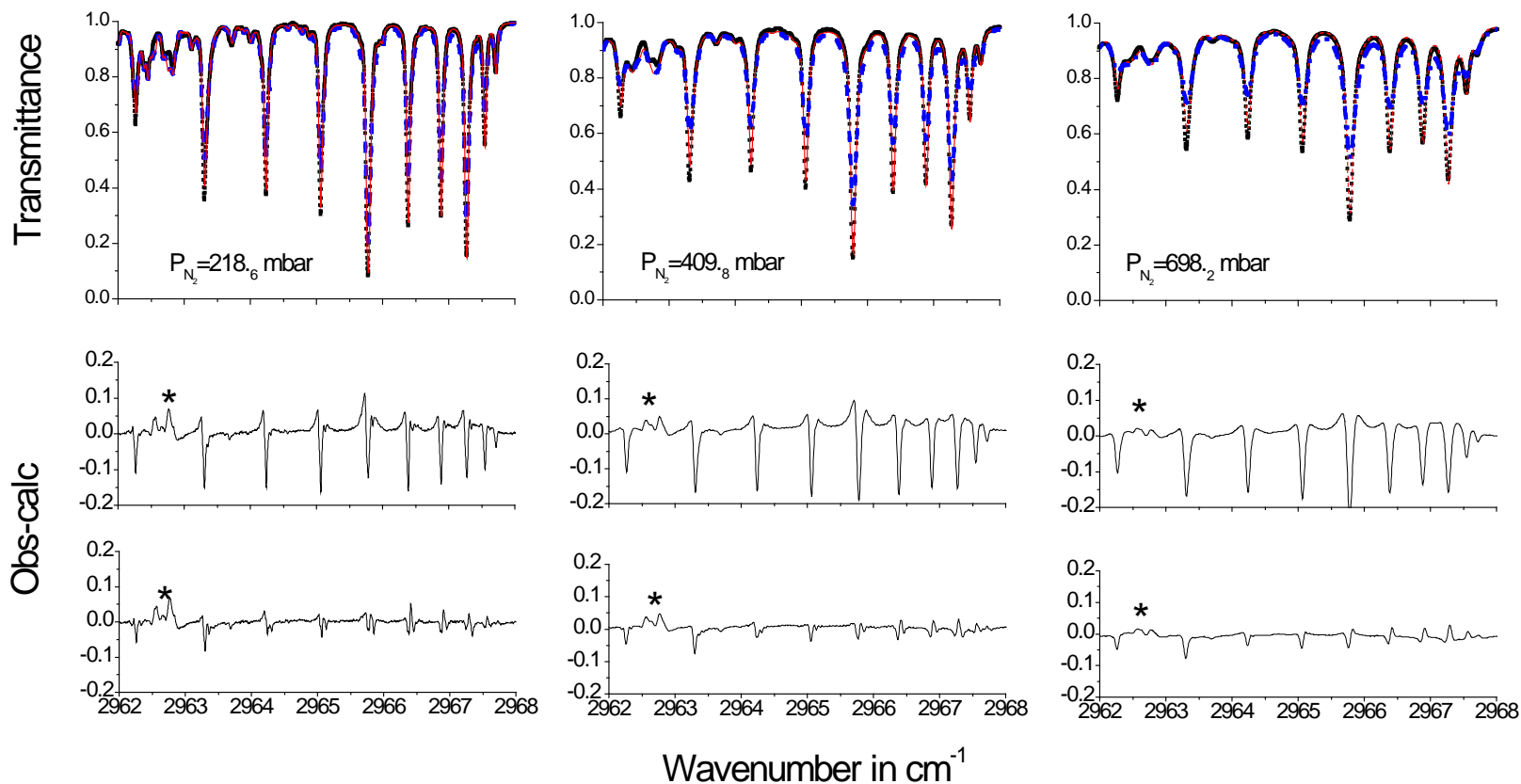
Comparison between the $\text{CH}_3\text{Cl}/\text{N}_2$ experimental spectra (■) of the oQ_6 sub-branch and those calculated without line mixing (---), with line mixing (—). The pressure of N_2 gas increases from left panel to the right one. The lower panels correspond to residuals of the fits showing the differences between the experimental spectra and calculated one using a sum of Lorentz profiles with (last panel) or without (first residual panel) taking into account line-mixing effects.



* ν_4 and $3\nu_6$ transitions taken into account in the calculation of the total absorption coefficient (Lorentz profiles). Spectroscopic data of these transitions are less accurate than the ν_1 ones.

Figure 4

Comparison between the $\text{CH}_3\text{Cl}/\text{N}_2$ transmission spectra in the oQ sub-branches region calculated without line mixing (---), with line mixing (—) and the experimental values (■). The pressure of N_2 gas increases from left panel to right. The lower panels correspond to residuals of the fits showing the differences between the experimental spectra and calculated one using a sum of Lorentz profiles with (last panel) or without (first residual panel) taking into account line-mixing effects.



* RQ_9 branch of the ν_4 band taken into account in the calculation of the total absorption coefficient (Lorentz profiles). Spectroscopic data of these transitions are less accurate than the ν_1 ones.

Figure 5

Comparison between the $\text{CH}_3\text{Cl}/\text{N}_2$ PNNL experimental spectra (■) of the oQ sub-branch and those calculated without line mixing (---), with line mixing (—). $P(\text{CH}_3\text{Cl}) = 1.10^{-6}$ atm, $P(\text{N}_2) = 1$ atm, $L = 100$ cm (experimental conditions from PNNL [22]). The panels of residuals show the differences between the experimental PNNL spectrum and a calculation without taking into account line-mixing effects (a) and by using our model to model line-mixing effects (b).

